Title

Stealth Immune Properties of Graphene Oxide Enabled by Surface-Bound Complement Factor H

Journal

ACS Nano, 10(11)

ISSN

1936-0851

Authors

Belling, Jason N
Jackman, Joshua A
Avsar, Saziye Yorulmaz
et al.

Publication Date

2016-11-22

DOI

10.1021/acsnano.6b05409

Peer reviewed

ACS NANO

www.acsnano.org

ARTICLE

Stealth Immune Properties of Graphene Oxide Enabled by Surface-Bound Complement Factor H

Jason N. Belling,[†,§,∥,#] Joshua A. Jackman,[†,#] Saziye Yorulmaz Avsar,[†] Jae Hyeon Park,[†] Yan Wang,[†] Michael G. Potroz,[†] Abdul Rahim Ferhan,[†] Paul S. Weiss,[§,∥,⊥] and Nam-Joon Cho*[,†,‡]

[†]School of Materials Science and Engineering, Nanyang Technological University, 50 Nanyang Avenue 639798, Singapore
[‡]School of Chemical and Biomedical Engineering, Nanyang Technological University, 62 Nanyang Drive 637459, Singapore
[§]California NanoSystems Institute, [∥]Department of Chemistry and Biochemistry, and [⊥]Department of Materials Science and Engineering, University of California, Los Angeles, Los Angeles, California 90095, United States

Supporting Information

ABSTRACT: With mounting evidence that nanomaterials can trigger adverse innate immune responses such as complement activation, there is increasing attention to the development of strategies that mask the complement-activating properties of nanomaterials. The current gold standard to reduce complement activation of nanomaterials is the covalent attachment of polymer coatings on nanomaterial surfaces, even though this strategy provides only moderate protection against complement activation. Akin to protein coronas that form on nanomaterial surfaces in physiological fluids, noncovalent strategies based on protein adsorption would offer a simplified, biomimetic approach to mitigate complement activation. Herein, we demonstrate that precoating graphene-based nanomaterials with purified, natural proteins enables regulatory control of nanomaterial-triggered complement activation. When the graphene-based nanomaterials were coated with complement factor H, nearly complete protection (>90% reduction) against complement activation (a "stealth effect") was achieved. By contrast, coating the nanomaterials with a passivating layer of bovine or human serum albumins achieved moderate protection (~40% reduction), whereas immunoglobulin G amplified complement activation by several-fold. Taken together, our results demonstrate that surface-bound factor H, as well as serum albumins, can prevent graphene oxide-triggered complement activation, thereby offering a facile approach to inhibit complement activation completely down to naturally occurring levels.

KEYWORDS: *factor H, serum albumin, graphene oxide, protein corona, protein coating, complement activation, immunomodulation*

Graphene-based nanomaterials possess remarkable electrical, mechanical, and optical properties and are increasingly utilized in biomedical applications such as drug delivery, imaging, and biosensing.[1−4] In particular, two-dimensional graphene oxide (GO) sheets exhibit attractive properties such as excellent dispersibility in water and organic solvents as well as an extremely high specific surface area, which opens the door to a multitude of surface functionalization possibilities.[5−7] Detailed understanding of how GO interacts with biological systems is of paramount importance for biomedical applications, especially in the context of immune compatibility for human safety.[8,9] To this end, a wealth of *in vitro* and *in vivo* studies have been performed in order to explore how graphene-based nanomaterials interact with the immune system, and a wide range of immune responses have been observed reflecting the rich milieu of influencing factors (*e.g.*, physicochemical properties of the graphene sample including impurities, cell type, and administration route).[10,11] For example, in one recent study, Sydlik *et al.* investigated the *in vivo* compatibility of GO and reduced graphene oxide (rGO) and identified that these nanomaterials elicit moderate immune responses akin to foreign body reactions, with quicker immune responses triggered by the reduced form.[12] Achieving deeper insight into how graphene-based nanomaterials, especially GO, interact with components of the immune system will not only advance fundamental knowledge but also contribute directly to realizing biomedical applications of GO.

Received: August 11, 2016
Accepted: October 28, 2016
Published: October 28, 2016

DOI: 10.1021/acsnano.6b05409
ACS Nano 2016, 10, 10161−10172

Arguably, one of the least-studied topics within this purview involves understanding how GO activates the complement system, which is part of the innate immune response.[13] Indeed, complement activation is one of the most important topics relating to nanomaterials in medicine[14−17] as various classes of nanoparticles and imaging agents are known to induce complement activation-related pseudoallergy (CARPA), which are acute hypersensitivity reactions that can be life threatening and even fatal.[18,19] Mechanistically, complement activation involves a highly orchestrated sequence of soluble and membrane-bound proteins and is triggered by the recognition of foreign particulates (*e.g.*, nanomaterials, bacteria) in the bloodstream.[20] It can proceed *via* one or more of three pathways (classical, alternative, and lectin), and the first step in all three pathways is the binding of complement proteins onto a target surface. This event triggers a signaling cascade that is centered around the complement C3 protein and can stimulate phagocytic clearance, formation of the lytic membrane attack complex (MAC), and release of anaphylatoxin byproducts that cause immune reactions.[21,22] There is an amplification loop within the alternative pathway that increases the overall complement response independent of which pathway was originally activated.[23] Along these lines, Feng *et al.* reported that GO activates the complement system, causing increases in anaphylatoxin levels.[24] Furthermore, Wibroe *et al.* determined that the oxidation state of GO influences the extent of complement activation, with more oxidized versions inducing greater complement activation.[25] Therefore, developing effective strategies to mask the complement-activating properties of GO is a key objective.

While soluble inhibitors have been utilized for regulating complement activation, their systemic administration can result in deleterious side effects, and hence, surface functionalization of nanomaterials with passivating molecules is a favorable approach that is actively being explored.[26,27] To date, various efforts to control the immune effects of GO include surface functionalization with antioxidants[28] and polymer coatings.[29] Tan *et al.* reported that covalently attached poly(ethylene glycol) (PEG) coatings on GO moderately reduced complement activation along with diminished release of anaphylatoxins.[30] While such results are promising, the levels of complement inhibition were suboptimal, and PEG-coated surfaces are known to activate the complement system in any case.[31−34] Since GO has a high protein-binding capacity, noncovalent protein coatings are another promising direction,[35] especially in light of growing evidence that supports the critical importance of the protein corona in shaping the biological identity of nanomaterials,[36−39] and such coatings have been shown to reduce GO-mediated cytotoxicity against human cells[40] as well as to improve the dispersibility of GO sheets in biological media.[41] However, to our knowledge, protein coatings have never been investigated in the context of mitigating GO-induced complement activation.

Much can be learned from the wealth of studies involving complement activation of another popular carbon nanomaterial, carbon nanotubes, as first reported by Salvador-Morales.[42] It was further identified that covalent modification (*e.g.*, coating carbon nanotubes with ε-caprolactam or L-alanine) could moderately reduce complement activation.[43] Importantly, it was observed that complement activation became more attenuated with increasing amounts of bound complement proteins (C1q and factor H), which spontaneously adsorbed onto the carbon nanotube surfaces when incubated in human serum. This finding suggested that precoating carbon nanotubes with purified serum proteins might prevent complement activation; however, attempts made with bovine serum albumin (BSA), human serum albumin (HSA), and human fibrinogen coatings were unsuccessful, likely due to incomplete protein adsorption across the carbon nanotube surfaces.[44−47] Pondman *et al.* reported that precoating carbon nanotubes with C1q fragments or factor H could partially reduce complement activation *via* the classical and alternative pathways, respectively.[48] Altogether, the results obtained in complement-activation studies on carbon nanotubes suggest that there is excellent potential to prevent nanomaterial-induced complement activation with protein coatings, but realization of this concept likely depends on the protein-binding capacity of a particular nanomaterial.[49]

From a broader perspective, there is significant interest in exploring ways to functionalize biomaterial surfaces with natural proteins that are involved in down-regulating the complement system, especially the complement factor H protein, which is the second-most abundant complement protein in plasma.[50,51] Andersson *et al.* coated polystyrene surfaces with factor H and identified that covalently tethered protein inhibited complement activation, whereas noncovalently bound protein was ineffective even though similar amounts of bound protein were achieved with both immobilization schemes.[52] Factor H has also been covalently attached to poly(ethylene oxide)-functionalized polystyrene surfaces, resulting in significantly reduced coagulation and complement activation.[53] Similar conjugation schemes have been adopted for coating factor H proteins onto the surface of mesenchymal stem cells, thereby protecting them from complement attack.[54] Mimicking how bacteria evade the human immune system by hijacking regulatory proteins, Wu *et al.* developed an alternative method to tether factor H-binding peptides covalently onto polystyrene surfaces, and when incubated in serum, factor H proteins became bound to this functionalized surface and significantly inhibited complement activation.[55,56] Based on the aforementioned studies, there is strong evidence supporting that factor H coatings are an excellent biomimetic strategy to reduce complement activation.[57] However, to date, covalent tethering of regulatory proteins and peptides was necessary in all cases in order to reduce the extent of complement activation triggered by biomaterial surfaces, highlighting the significant and unmet potential to develop complement inhibiting surfaces based on noncovalent protein attachment.

Herein, we report a simple, noncovalent functionalization method to endow GO nanomaterials with stealth immune properties based on surface-bound protein coatings. Four different proteins were selected for investigation: BSA, HSA, factor H, and immunoglobulin G (IgG). BSA and HSA are structural homologues that were selected because serum albumins are the most abundant proteins in blood plasma and promote favorable biological activities when coated on GO (*e.g.*, reduced cytotoxicity). Factor H was selected because it is the most widely studied complement regulatory protein for surface-coating applications, and it is expected to inhibit complement activation provided that the bound form is functionally active. On the other hand, IgG is an antibody that is involved in complement-mediated pathogen clearance, and its surface-bound form is known to *promote* complement activation.[58] Hence, the tested proteins have a wide range of biological functionality, and we demonstrate that the interaction between GO and the complement system can be

DOI: 10.1021/acsnano.6b05409
ACS Nano 2016, 10, 10161−10172

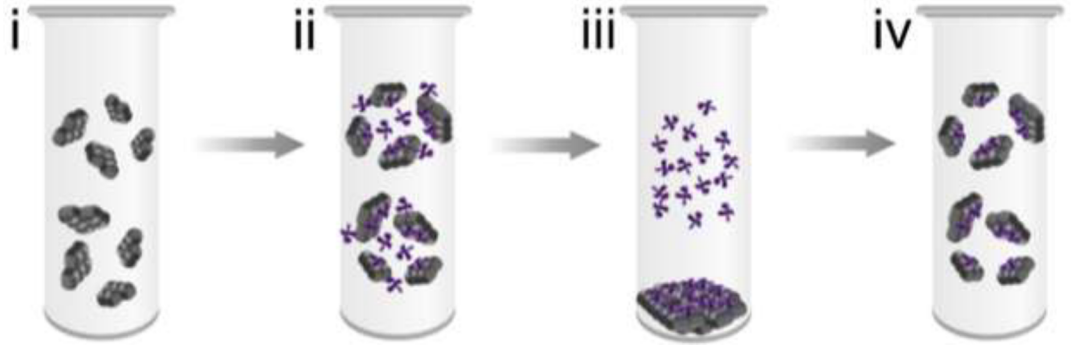

Figure 1. Schematic illustration of process to coat single-sheet graphene oxide flakes with adsorbed protein layers. (i) Graphene oxide (GO) flakes are dispersed in deionized water. (ii) Protein is added to the GO solution, and the mixture is incubated at elevated temperature (37 °C) in order to facilitate protein adsorption. (iii) A centrifugation step is performed in order to separate protein-coated GO flakes (pellet) from free protein (supernatant). The supernatant is removed by aspiration. (iv) Protein-coated GO flakes are redispersed in fresh PBS and form a stable suspension.

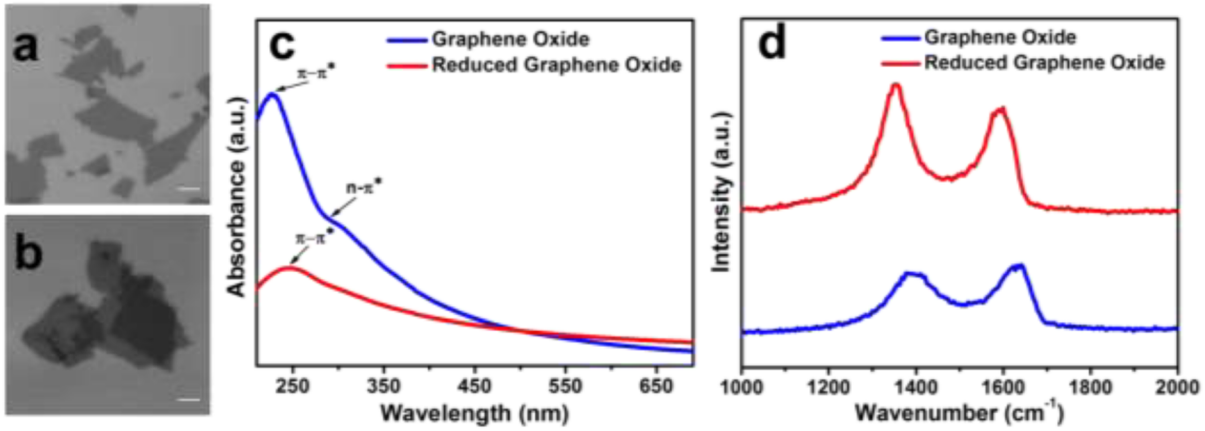

Figure 2. Morphological and chemical characterization of graphene oxide and reduced graphene oxide sheets. Scanning electron microscopy micrographs of (a) graphene oxide (GO) and (b) reduced graphene oxide (rGO) sheets. Scale bars are 1 μm. (c) UV−vis spectra of GO and rGO with labels denoting specific bonding orders. (d) Raman spectra of GO and rGO with indicated D and G bands.

modulated based on the identity of the protein coating. With rapid advances in scientific knowledge about how protein coatings modulate the biological activities of nanomaterials,[37,59−63] the present findings reinforce the notion that engineering synthetic protein coronas based on complement biology can greatly improve the immune compatibility of nanomaterials, particularly in the context of mitigating nanomaterial-induced complement activation.

RESULTS AND DISCUSSION

Protein-Coating Strategy. We begin by outlining the steps taken to prepare a complement-inhibiting protein coating on the surface of GO. A noncovalent functionalization approach was utilized that takes advantage of spontaneous protein adsorption onto individual GO flakes in solution. In this regard, GO is an ideal nanomaterial because it exhibits a high protein-binding capacity,[41,64−66] and adsorbed proteins are known to remain tightly bound.[67−69] Figure 1 presents a schematic illustration of the preparation scheme. GO and protein are incubated together in phosphate-buffered saline (PBS) for 2 h at 37 °C, during which time proteins adsorb onto the GO surface. To remove unbound protein, the protein-coated GO samples are centrifuged, resulting in a sedimented pellet with protein-coated GO and the residual supernatant contains unbound protein. The supernatant is discarded, and fresh aqueous buffer solution is added in order to resuspend the pellet. As adsorbed proteins remain strongly bound to GO, this approach enables a simple, yet effective approach to prepare protein-coated GO sheets.

Preparation and Characterization of Graphene Oxide Nanomaterials. As the oxidation state of GO is known to influence its complement-activating properties,[25] we investigated the formation of protein coatings on two different GO preparations, specifically GO sheets prepared by Hummers' method and rGO sheets that underwent an additional reduction step with hydrazine (see the Experimental Methods and Materials). It is known that GO disperses well in aqueous solution, while rGO has tendencies to wrinkle and aggregate.[70] Scanning electron microscopy (SEM) micrographs show the formation of single-sheet GO flakes with an average surface area of 1.89 ± 0.19 μm^2 per sheet (Figure 2a). As expected, the SEM micrographs also revealed greater aggregation of rGO sheets (Figure 2b). Atomic force microscopy (AFM) experiments confirmed the single-sheet morphology of GO flakes, with a sheet thickness of ∼1 nm (Figure S1). On the other hand, rGO sheets display a wrinkled, folded morphology, which is consistent with aggregation.

As shown in Figure 2c, ultraviolet−visible (UV−vis) spectroscopic measurements display the characteristic shoulder of GO at 230 nm corresponding to the $\pi-\pi^*$ bonding of C═C

DOI: 10.1021/acsnano.6b05409
ACS Nano 2016, 10, 10161−10172

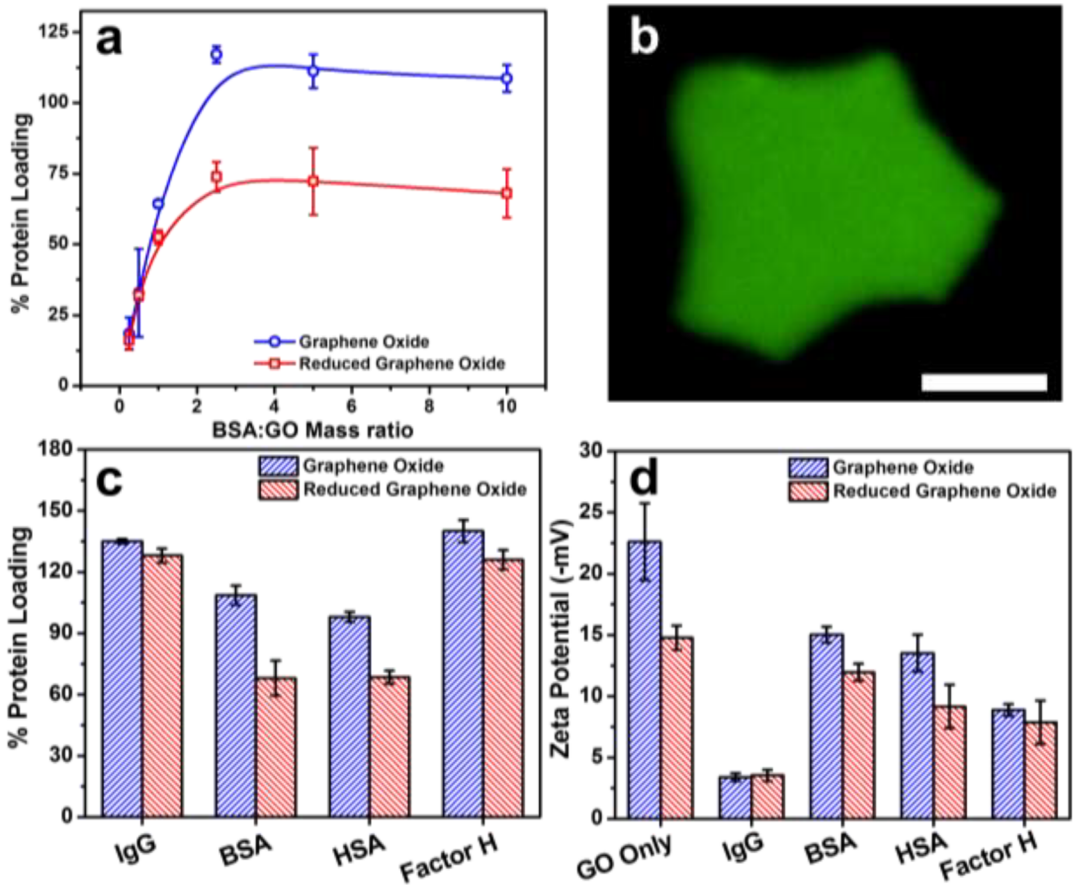

Figure 3. Protein coatings on graphene-based nanomaterials. (a) Protein loading percentage (ratio of loaded protein mass and nanomaterial mass × 100%) for bovine serum albumin (BSA) adsorption onto graphene oxide (GO) (blue circles) and reduced graphene oxide (rGO) (red square), as determined by a bicinchoninic acid protein assay. Data are expressed as mean and standard deviation from n = 3 experiments. (b) Fluorescence micrograph of fluorescein isothiocyanate-labeled BSA adsorbed onto a single GO flake. After the coating procedure was completed, the protein-coated flake was deposited on a glass substrate for imaging. The scale bar is 5 μm. (c) Protein loading percentage of different serum proteins onto GO and rGO. Data are expressed as mean and standard deviation from n = 3 experiments. (d) Zeta potential values of pristine and protein-coated GO and rGO flakes. Data are expressed as mean and standard deviation from n = 5 experiments.

aromatic rings and the 300 nm band arising from n−π* transitions of C═O bonds.[71] In addition, successful GO reduction is verified by a redshift of the 230 nm band to 260 nm and disappearance of the 300 nm band due to the absence of C═O bonds.[72] The Raman spectrum of GO shows two characteristic intensity (I) peaks (D and G bands), and the I_D/I_G ratio was 0.95, which is consistent with GO samples (Figure 2d). Likewise, the I_D/I_G ratio for rGO increased to 1.1 because there is an increase in the number of defects in the carbon lattice for hydrazine-reduced GO.[73] Fourier transform infrared (FTIR) spectral measurements were conducted in transmission mode and revealed significant decreases in the intensities of the hydroxyl stretching band around 3400 cm^{-1} and the carboxyl stretching band at ∼1630 cm^{-1} for rGO (Figure S2).[74] Moreover, for rGO, the intensity of the bending vibration of the C−OH group at ∼1360 cm^{-1} was diminished, while the intensity of the C−O stretching band at ∼1000 cm^{-1} increased.[75] Hence, morphological and chemical characterization efforts verify successful GO and rGO preparation toward evaluation of protein coatings.

Optimization of Protein Coating. We first investigated the effects of protein/nanomaterial mass ratio on protein loading efficiency and used BSA protein for the initial optimization experiments. The nanomaterial (GO or rGO) mass was fixed at 25 μg, and the amount of BSA varied accordingly. The BSA protein loading was determined by employing a bicinchoninic acid (BCA) assay in order to measure the bulk protein concentration.[76] Fixed amounts of nanomaterial and BSA in PBS solution were incubated for 2 h at 37 °C, followed by centrifugation in order to separate unbound protein in the supernatant from the sedimented, protein-coated nanomaterial samples. The amount of loaded protein was determined based on calculating the difference between the stock BSA concentration and the BSA concentration in the residual supernatant (see Figure S3). These measurements enabled us to calculate the protein loading percentage by the following equation: $[(C_{BSA\text{-}Total} - C_{BSA\text{-}supernatant})/C_{GO}] \times 100$.

Figure 3a presents the protein loading as a function of the protein/nanomaterial mass ratio, which was varied during the incubation step. For GO samples, the loading value reached saturation around 2.5:1 BSA/GO mass ratios and beyond. The measured saturation value (∼110%) is in good agreement with literature reports[40,49] and confirms the high protein-loading capacity of GO as compared to other carbon-based nanomaterials (*e.g.*, carbon nanotubes). By contrast, significantly less BSA protein was adsorbed onto rGO surfaces, with the loading value reaching only ∼75% at saturation indicating that the

DOI: 10.1021/acsnano.6b05409
ACS Nano 2016, 10, 10161−10172

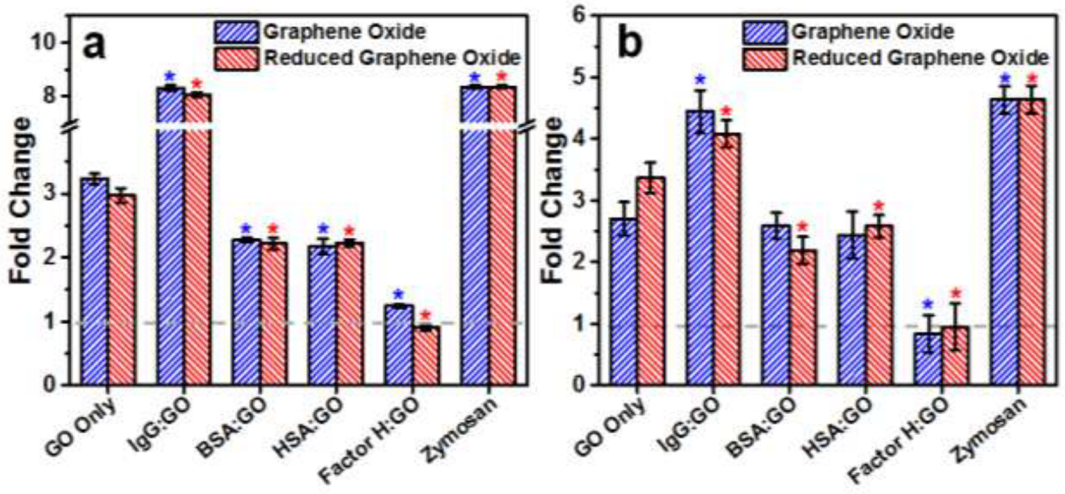

Figure 4. ELISA measurements of graphene oxide-induced membrane attack complex generation. (a) Influence of protein coatings on graphene oxide induced membrane attack complex generation in normal human serum. Negative control samples without protein (labeled GO only) and zymosan positive control were also tested in parallel experiments. The fold change in sC5b-9 levels was determined relative to complement activation in aqueous buffer solution without nanomaterial or protein (denoted by dashed line). (b) Equivalent measurements were conducted in EGTA-treated normal human serum. Data are expressed as mean and standard deviation from $n = 3$ experiments.

protein loading capacity of GO is higher than that of rGO.[24] This lower value is consistent with less available surface area due to rGO forming small aggregates in buffer solution.[49]

To verify protein adsorption onto individual GO flakes, confocal microscopy experiments were conducted using protein-coated GO samples.[77] Fluorescein isothiocyanate (FITC)-labeled BSA was incubated for 2 h with GO in a 10:1 weight ratio, centrifuged, and washed extensively in order to remove unbound BSA. Then, the protein-coated GO sample was deposited on a clean glass substrate for imaging. Figure 3b shows that the protein-coated GO sample presents bright fluorescence with a nonfluorescent background. In contrast, uncoated GO is not fluorescent under the same illumination and detection settings, confirming that the fluorescence signal arises from the protein coating. Moreover, line profiles of the fluorescence intensity across the protein-coated GO surface indicate that the fluorescence intensity across a single protein-coated GO sheet is uniform (Figures S4 and S5). Taken together, using BSA as a model protein, we identified that the 10:1 protein/nanomaterial mass ratio is a suitable condition for the incubation step and further demonstrate selective immobilization of protein on the GO surface.

To investigate the coating of other tested proteins on GO and rGO surfaces, additional BCA assay experiments were conducted (Figure 3c). The appropriate protein, BSA, HSA, IgG, or factor H, was incubated for 1 h with GO or rGO in a 10:1 weight ratio and then centrifuged in order to separate unbound protein from coated protein, thereby enabling indirect measurement of the amount of loaded protein. In the GO case, the BSA and HSA coatings had similar loading percentages (~100−110%), while IgG and factor H exhibited even greater loading, with values reaching 140%. Figure 3d presents the zeta potential values for pristine GO and rGO and the protein-coated variants thereof. The zeta potential values of GO and rGO were −22.6 ± 3.1 mV and −14.8 ± 1.0 mV, respectively, which are attributed to ionization of functional groups and agree well with literature values.[70,78] Interestingly, protein coatings resulted in decreased zeta potential values, with BSA and HSA coatings having similar effects. Albumin-coated GO and rGO had zeta potential values of *ca.* −15 and −10 mV, respectively, indicating only minor changes in surface charge.[41] On the other hand, factor H- and IgG-coated samples had greater reductions in zeta potential values to *ca.* −8 and −3 mV, respectively. Altogether, the data confirm the successful preparation of protein-coated GO with an optimized protocol that we carried forward to evaluate for complement-inhibiting activities.

Inhibition of Total Complement Activation. One of the most widely used *in vitro* markers of total complement activation is the MAC, which is generated as part of complement activation across all three pathways. It provides a key indicator for evaluating the complement-activating properties of a nanomaterial.[16] Pristine and protein-coated GO samples were incubated in normal human serum, and the generated levels of the MAC (sC5b-9) were measured by an enzyme-linked immunosorbent assay (ELISA) (Figure 4). As part of innate host defense, low levels of complement activation are a naturally occurring process and baseline levels were recorded in normal human serum (Figure 4a). In the presence of pristine GO or rGO, there was a nearly 3-fold increase in sC5b-9 generation. Compared to the pristine samples, IgG-coated samples strongly activated complement by more than 200%, behaving similarly to the zymosan positive control. On the other hand, the rest of the protein coatings reduced sC5b-9 generation.

The BSA and HSA protein coatings had similar performances, yielding ~40% inhibition as compared to pristine samples. Strikingly, the factor H-coated samples achieved >90% inhibition, as compared to pristine samples, demonstrating nearly complete prevention of complement activation. The experiments were also conducted in EGTA-treated serum, in which only the alternative pathway is known to be active (Figure 4b).[79] The IgG-coated samples again provoked sC5b-9 generation, while the factor H-coated samples reduced sC5b-9 generation down to background levels, effectively demonstrating 100% inhibition of complement activation down the alternative pathway. In contrast, the BSA- and HSA-coated samples were less effective, with inhibition levels ranging

DOI: 10.1021/acsnano.6b05409
ACS Nano 2016, 10, 10161−10172

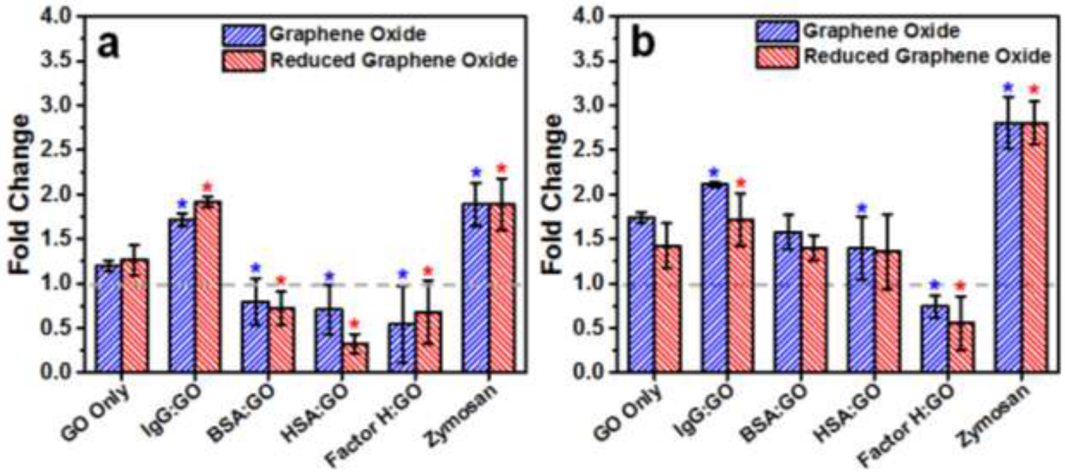

Figure 5. ELISA measurements of graphene oxide-induced C3 cleavage. (a) Influence of protein coatings on graphene oxide (GO)-induced C3a generation in normal human serum. Negative control samples without protein (labeled GO only) and zymosan positive control were also tested in parallel experiments. The change in C3a levels was determined relative to complement activation in aqueous buffer solution without nanomaterial or protein (denoted by dashed line). (b) Equivalent measurements were conducted in EGTA-treated normal human serum. Data are expressed as mean and standard deviation from n = 3 experiments.

between 5 and 35%, compared to pristine samples. Taken together, these findings demonstrate that factor H is a highly effective coating to mitigate GO-induced complement activation.

In addition, the levels of C3a generated were measured by ELISA measurements, as shown in Figure 5. Released from the C3 convertase as part of complement activation, the C3a peptide is an inflammation-causing anaphylatoxin, which serves as another marker of total complement activation.[80] In normal human serum, pristine GO and rGO had a 20% increase in C3a release over background levels, while IgG-coated samples, and the zymosan positive control, induced significantly increased C3a release (~80−100% increase) compared to pristine samples (Figure 5a). A surprising observation was that GO samples coated with factor H or one of the serum albumins not only prevented complement activation but also effectively inhibited C3a release well below baseline levels. In EGTA-treated serum, similar results were obtained; however, there was a pronounced decrease in the inhibitory effectiveness of BSA- and HSA-coated samples (Figure 5b). In marked contrast, factor H coatings again inhibited C3a release, consistent with the notion that surface-bound factor H is functionally active as a complement inhibitor. Overall, the data supports that factor H-coated GO nanomaterials largely avoid activating the complement system based on only marginal increases in MAC generation and inhibition of C3a anaphylatoxin release.

Modulation of Specific Complement Pathways. To understand how protein-coated GO nanomaterials bypass the alternative and classical pathways of complement activation, the generation of additional complement markers was measured. When the alternative pathway is activated, complement factor D cleaves complement factor B, yielding an inactive Ba fragment and a proteolytic Bb fragment that forms a complex with C3b known as the C3bBb convertase.[81] Since this convertase cleaves the C5 protein leading to MAC formation,[82] the concentration of generated Bb fragments is an important indicator of the extent of complement activation along the alternative pathway. Figure 6 presents the levels of Bb generated, as measured by ELISA measurements. Compared to baseline levels, Bb generation induced by pristine GO or

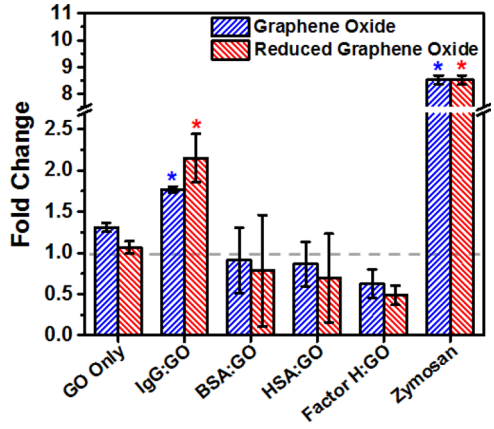

Figure 6. ELISA measurements of graphene oxide-induced activation of the alternative pathway. Influence of protein coatings on graphene oxide (GO) induced Bb generation in normal human serum. Negative control samples without protein (labeled GO only) and zymosan positive control were also tested in parallel experiments. The change in Bb levels was determined relative to complement activation in aqueous buffer solution without nanomaterial or protein (denoted by dashed line). Data are expressed as mean and standard deviation from n = 3 experiments.

rGO was increased by 10−30%. However, appreciable increases in Bb production (70−120% increase) were observed for IgG-coated samples. On the other hand, BSA- and HSA-coated samples strongly inhibited Bb production down to baseline levels, while factor H-coated samples prevented Bb production below baseline levels. This finding offers further evidence that surface-adsorbed factor H is strongly inhibitory against the alternative pathway, likely stymieing the amplification loop of the alternative pathway.

To determine the role of nonalternative pathways, *i.e.*, the classical and lectin pathways, in the complement response to protein-coated GO and rGO, the levels of C 4d, a split product of C4 that is used as a diagnostic biomarker and believed to play a role in mediating inhibitory effects on immune cells,[83] were determined by ELISA measurements, as shown in Figure 7. Pristine GO and rGO caused an 80% increase in C 4d

DOI: 10.1021/acsnano.6b05409
ACS Nano 2016, 10, 10161−10172

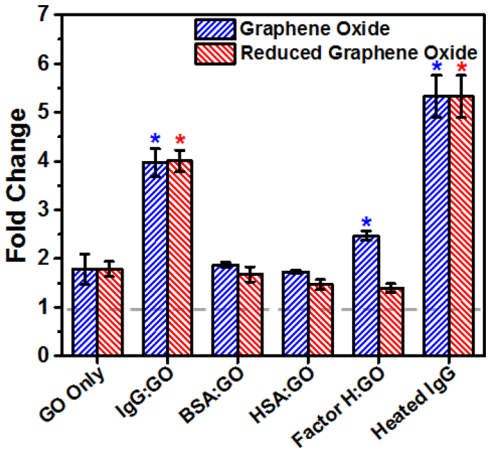

Figure 7. ELISA measurements of graphene oxide induced activation of nonalternative (classical and lectin) pathways. Influence of protein coatings on graphene oxide (GO) induced C 4d generation in normal human serum. Negative control samples without protein (labeled GO only) and heat-treated IgG positive control were also tested in parallel experiments. The change in C 4d levels was determined relative to complement activation in aqueous buffer solution without nanomaterial or protein (denoted by dashed line). Data are expressed as mean and standard deviation from n = 3 experiments.

production, while IgG-coated samples induced almost 3-fold higher production than pristine samples. The latter observation is in good agreement with results obtained for the heat-treated IgG aggregates, which serve as the positive control for this experiment.[58] In contrast, both BSA and HSA coatings had negligible effects on C 4d generation. While the factor H coating on rGO also had a negligible effect, one surprising finding was that the factor H coating on GO increased C 4d production by around 30%. Considering that multiple lines of evidence strongly support that factor H-coated GO nanomaterials do not induce complement activation beyond naturally occurring levels, this finding demonstrates that inhibiting the alternative pathway is the key process to prevent excessive complement activation due to the fact that the alternative pathway contains the amplification loop that translates initial recognition-level events in each pathway into a concerted immune response. Taken together, these findings establish that protein-coated graphene nanomaterials can be readily fabricated using noncovalent self-assembly, and complement activation or inhibition can be controllably tuned based on protein identity. Importantly, we demonstrate that factor H-coated graphene nanomaterials can effectively prevent complement activation.

The demonstrated capability of albumin and factor H coatings to cloak GO and to mitigate complement activation supports that there are at least two ways in which these coatings work. The first effect likely relates to steric blocking as the protein coating acts as a passivating layer in order to prevent complement proteins from interacting with GO (*e.g.*, as for serum albumins). At the same time, surface-bound proteins involved in regulating complement activation may have additional effects, as demonstrated by inhibition of complement activation in the case of surface-bound factor H coatings. Indeed, the case of factor H is of particular interest because there have been extensive efforts to develop factor H coatings, with limited success. As described in the introduction, noncovalent deposition of factor H onto hydrophobic polystyrene surfaces was unsuccessful at preventing complement activation,[52] in turn inspiring more sophisticated efforts to tether purified factor H[53] covalently or to recruit endogenous factor H to surfaces.[55] However, it is well-known that adsorption of the same protein onto hydrophobic surfaces *versus* hydrophilic surfaces proceeds in different ways, and these differences can be reflected in the orientation and conformational properties of the adsorbed protein.[84] The fact that noncovalent deposition of factor H on polystyrene does *not* result in functional, surface-adsorbed factor H does not exclude the possibility that surface-adsorbed factor H on hydrophilic surfaces, or at least some subset thereof, could retain function as a complement inhibitor, as demonstrated here. Furthermore, early attempts to utilize noncovalent protein deposition as a means of mitigating nanomaterial-induced complement activation had limited success, although it should be emphasized that those studies utilized carbon nanotubes, which have significantly lower protein binding capacities than GO (*vide supra*). As such, we demonstrate that noncovalent deposition of factor H on a hydrophilic surface, namely GO sheets, is successful at mitigating complement activation, and this approach should be explored further for nanomaterials and more generally for the surfaces of biomaterials.

In order to explain why factor H coatings are so effective at not only preventing complement attack but also lowering basal levels of complement activation, we note that factor H is a known complement inhibitor that regulates the amplification loop of the alternative pathway.[85] Specifically, factor H binds to complement C3b fragments and inhibits formation of the C3bBb convertase, which is necessary for propagating the amplification response, thereby inhibiting downstream (terminal) events in the complement cascade (*e.g.*, MAC formation, C5a generation).[50] Therefore, in order to ascertain if surface-bound factor H on GO maintains functional activity, we performed a direct cofactor assay in which factor H-coated GO or BSA-coated GO was incubated in buffer containing C3b (104 kDa) and factor I. Functionally active factor H is a cofactor for factor I-mediated C3b cleavage, yielding inactivated C3b (iC3b) protein.[86] Indeed, by employing Western blot analysis, we observed that surface-bound factor H retains functional activity based on iC3b generation and the resulting fragment thereof, with observed behavior similar to that of the soluble factor H control alone (Figure S6). By contrast, surface-bound BSA did not facilitate iC3b generation. The findings reinforce our foregoing observations that serum albumin coatings mitigate GO-induced complement activation by a passivating effect, whereas factor H coatings not only exhibit a passivating effect but also maintain some degree of functional activity that mirrors the natural regulatory role of soluble factor H. Within this context, one significant advantage of mitigating complement activation at the amplification stage is that complement-mediated immune surveillance is still possible at the initiation stages of complement activation preceding the amplification loop.[87] Indeed, there has been growing interest in complement therapies directed against complement C3 protein and fragments thereof (*e.g.*, C3b protein), and localized inhibition of complement activation due to factor H coatings is an attractive strategy that avoids potential complications from systemically administered C3/C3b inhibitors.[88]

In the broader context of nanomaterials, our findings demonstrate that protein-coating strategies can provide an effective means to inhibit nanomaterial-triggered complement activation. Considering that all of the proteins evaluated in this

DOI: 10.1021/acsnano.6b05409
ACS Nano 2016, 10, 10161−10172

study are found in abundance in blood, the feasibility of extending this approach beyond purified proteins to physiological fluids warrants attention. Indeed, incubating GO in fetal bovine serum has previously led to the formation of a natural protein corona that mitigates GO-induced cytotoxicity.[40] However, in the case of preventing complement attack, recent evidence points to the importance of using purified proteins because this strategy offers greater control over the protein composition on the nanomaterial surface.[89] In particular, Xu *et al.* identified that IgG is the main serum protein that comprises the natural corona formed on GO.[29] On the basis of our findings, an IgG-coated GO *stimulates* complement activation as compared to pristine GO, and hence, a natural protein corona with IgG as the main constituent would likely be ineffective, at least in the case of GO. Therefore, precoating GO with purified proteins or combinations thereof likely represents the best opportunity to prevent complement attack, and the balance of natural *versus* biomimetic corona strategies should be weighed for other nanomaterials depending on the protein composition of natural coronas that spontaneously form on them. For example, Yu *et al.* characterized the relative fraction of adsorbed proteins within the protein corona that formed on glycopolymer-modified nanoparticles in physiological fluids and discovered that nanoparticles that adsorbed more factor H induced lower levels of complement activation.[90] Lastly, we note that the specific composition of the protein corona likely shifts from a homogeneous coating of a single protein to a more diverse milieu of proteins when the GO nanomaterial is exposed to physiological fluids, as reported in other recent work.[91−93] While our findings identify that factor H and serum albumin coatings both prevent GO-induced complement activation to differing extents, understanding the implications of these findings in terms of the final corona composition is an outstanding subject for future work, especially in the context of identifying other protein coatings that might help recruit endogenous factor H to the nanomaterial surface. In line with the aforementioned reports identifying a correlation between low complement activation and the amount of endogenous factor H adsorbed onto a nanomaterial surface as part of the corona, our observation that surface-bound factor H can serve as a cofactor to promote iC3b generation supports that factor H itself is an important part of the corona composition.

Moreover, in terms of biomimetic strategies to precoat nanomaterials with regulatory proteins, there is a significant opportunity to explore how factor H and its constructs (*i.e.*, mini-factor H), as well as other complement inhibitors (*e.g.*, vitronectin, compstatin, clusterin), influence not only complement activation but also other aspects of the innate immune response as well as minimize nonspecific cellular uptake, potentially enabling truly comprehensive stealth immune properties. Indeed, mini-factor H is a promising therapeutic agent for treating complement-related diseases[94] with superior inhibitory activity against complement activation as compared to factor H, and Mészáros *et al.* recently demonstrated in *in vitro* experiments that exogenous factor H and mini-factor H can inhibit complement activation induced by liposomal and micellar drugs as well as by the therapeutic antibody rituximab.[95] However, one challenging aspect thus far in the clinical translation of mini-factor H constructs has been their short serum half-lives.[96] Coating complement inhibitors onto nanomaterial surfaces as presented here offers a simple approach to not only regulate innate immune responses triggered by the nanomaterial itself but could also potentially lead to drug delivery platforms that improve the pharmacokinetic and pharmacodynamic properties of complement inhibitors.

CONCLUSIONS AND PROSPECTS

In this work, we have shown that protein coatings on GO enable highly effective mitigation of nanomaterial-induced complement activation in a manner that strongly depends on the protein identity. Compared to previous attempts with polymeric coatings, our results demonstrate that protein coatings offer a superior and simpler functionalization approach that can be harnessed either to down-regulate or to up-regulate the complement system. In particular, both albumin and factor H coatings demonstrated significant protection against complement attack, with surface-adsorbed factor H functioning effectively as a complement inhibitor that conferred stealth immune properties. Such approaches should be broadly applicable to two-dimensional nanomaterials with high protein binding capacities along with other biomaterial surfaces. Looking forward, there is enormous promise at the interface of nanomaterials and complement biology, with broad implications for a wide range of biomedical applications.

EXPERIMENTAL METHODS AND MATERIALS

Reagents. The BSA, FITC-conjugated bovine serum albumin, HSA, and IgG protein reagents were obtained from Sigma-Aldrich and stored at 4 °C. Purified human factor H, factor I, C3b, and iC3b were obtained from Complement Technology (Tyler, TX) and stored at −80 °C. Normal human serum and preactivated zymosan saline were also obtained from Complement Technology and stored at −80 °C. Complement iC3b (neoAntigen) antibody (013III-1.16) (catalog no. MA1-82814) was the primary mouse monoclonal antibody for iC3b and was obtained from Thermo Fisher Scientific. The secondary antibody, a goat antimouse IgG (H+L)−HRP conjugate (catalog no. 170-6516), was purchased from Bio-Rad Laboratories (Singapore). All other reagents were purchased from Sigma-Aldrich or Bio-Rad Laboratories and were of analytical grade.

Preparation of Graphene Oxide and Reduced Graphene Oxide. A commercially synthesized GO solution from Sigma-Aldrich (catalog no. 777676) was prepared as a stock concentration of 4 mg/mL in deionized (DI) water. For the chemical reduction of GO, the stock solution was diluted to 0.5 mg/mL with DI water to a final volume of 5.616 mL and heated to 60 °C in a water bath. Twenty microliters of a 1:10 (v/v) dilution of hydrazine monohydrate was then incubated in the heated GO solution for 1 h. After incubation, the solution was removed from the water bath and centrifuged at 16000*g* for 30 min. Sedimented rGO was separated from the supernatant in order to remove any residual hydrazine. The rGO was then redispersed in DI water or PBS depending on the experiment.

Materials Characterization. The GO sheets were drop-casted onto clean silicon dioxide substrates for material characterizations. The substrates were first cleaned by rinsing with acetone, 2-propanol, methanol, and water and were dried with a gentle stream of nitrogen gas and 2 h treatment in a Novascan PSD benchtop UV-ozone cleaner (Ames, IA). Next, 3 μL of 50 μg/mL GO or rGO in deionized water was drop-casted onto the clean substrate and allowed to dry overnight at room temperature. The SEM characterization was performed using a JEOL FESEM 7600F instrument at an accelerating voltage of 7 kV and images were taken at 6000× magnification. Atomic force microscopy (AFM) experiments were conducted using a Park Systems NX-Bio instrument (Suwon, South Korea) in contact mode with a 1 Hz scan speed and a NT-MDT CSG01 silicon cantilever (Tempe, AZ) with a spring constant of 0.07 N/m. UV−vis spectra were collected using a PerkinElmer Lambda 35 ES UV/vis spectrophotometer (Waltham, MA). Raman spectra were recorded using a WITec Alpha300RSA (Ulm, Germany) with an excitation laser wavelength of 488 nm. Infrared spectra were collected using a Bruker VERTEX 70

DOI: 10.1021/acsnano.6b05409
ACS Nano 2016, 10, 10161−10172

Fourier transform infrared spectrometer (Billerica, MA) that was operated in transmission mode over the range from 4500 to 500 cm^{-1} with a scanning resolution of 2 cm^{-1} with 100 repetitive scans. Samples for FTIR analysis were prepared by mixing solutions with KBr and preparing pellets with a hydraulic press.

Protein Loading. Proteins were hydrated in PBS at a concentration of 1 mg/mL, and appropriate volumes were incubated with 0.5 mL of 0.05 mg/mL GO and rGO diluted in PBS, fixing the nanomaterial mass at 25 μg. Samples were incubated at 37 °C for 2 h and then centrifuged at 16,000g for 30 min. The supernatant was removed, and the pellet was suspended in fresh PBS, while the supernatant was characterized by using a bicinchoninic acid (BCA) protein assay from Thermo Scientific (Pierce BCA protein assay kit). A 25 μL aliquot of protein supernatant was measured in triplicate in order to determine the unbound protein amount, from which the bound protein amount was determined using standard curves.

Zeta Potential Measurements. The electrophoretic mobility of pristine and protein-coated GO sheets in solution was determined by laser Doppler velocimetry and phase analysis light scattering measurements. A Malvern Zetasizer Nano ZS ZEN 3600 (Malvern Instruments Inc., UK) with a 633 nm wavelength laser was used for all measurements. The measurements were conducted in a 10 mM Tris (pH 7.5) buffer solution with 10 mM NaCl. The temperature of all experiments was set at 24 °C.

Fluorescence Confocal Laser Scanning Microscopy. The FITC-labeled BSA was first incubated with GO at a protein/nanomaterial ratio of 10:1 (saturation condition) in PBS and then centrifuged, after which the supernatant was discarded and the precipitate was redispersed in PBS. Then, 3 μL of FITC-BSA-loaded GO was drop-casted onto glass microscope slides. Each slide was precleaned with acetone, 2-propanol, and deionized water followed by a 2 h ozone treatment. Fluorescence CLSM imaging was performed using a Carl Zeiss LSM710 confocal microscope (Oberkochen, Germany). A drop of mounting medium (Vecta-shield) was added on top of the drop-cast sample followed by a coverslip. Images were collected under the following conditions: laser excitation line of 488 nm at 11.1% power; EC Plan-Neofluar 100 × /1.3 Oil M27 objective lens; pinhole of 175 μm; emission filter of 416−477 μm; image size of 28.3 μm × 28.3 μm, 1024 × 1024 pixels; and pixel dwell time of 177 μs. Images were processed using the ZEN 2008 Light Edition software package.

ELISA Assays. MicroVue sC5b-9 Plus EIA, Bb Plus EIA, C 4d EIA, and C3a Plus EIA kits were purchased from Quidel (San Diego, CA). Before the experiments, protein coatings were formed on GO and rGO sheets following the procedures described above (10:1 mass ratio), with a fixed nanomaterial mass of 15 μg. The samples were then centrifuged, and the supernatant was discarded while the precipitated nanomaterial was resuspended in fresh PBS. After redispersion, 10 μL of the sample was mixed with 40 μL of normal or EGTA-treated human serum in a 1:4 volumetric ratio, with final nanomaterial concentrations of 30 μg/mL in serum. The samples were incubated for 60 min at 37 °C and then transferred to an ice bath along with 25 mM EDTA addition to stop complement activation. Zymosan was used as a positive control for most experiments and was incubated in serum at a final concentration of 1 mg/mL. The only exception was the C 4d kit, for which the positive control was heat-aggregated IgG, which was previously incubated in PBS at 70 °C for 30 min and then subsequently diluted in normal human serum to a final concentration of 1 mg/mL. All kits were followed according to the manufacturer's instructions, measurements were conducted in triplicate, and the results are expressed as the mean ± standard deviation. Statistical significance was evaluated by one-way analysis of variance (ANOVA) followed by the Tukey test, and the values were compared to those of the GO or rGO-only measurements. Statistical analysis was conducted using the OriginPro 9 software program (OriginLab Corporation, Northampton, MA), and a P value of less than 0.05 was considered to be statistically significant (*).

SDS-PAGE and Western Blot Analysis. Protein-coated GO samples were suspended in 0.5 mL of PBS and then mixed together with 0.5 mL of purified factor I (0.005 mg/mL) and 0.5 mL of purified C3b (0.05 mg/mL) sequentially. The mixture was incubated at 37 °C for 30 min. After incubation, the samples were centrifuged at 16000g for 30 min, and the supernatant from each sample was collected for Western blot analysis. The supernatants were mixed with 4× Laemmli sample buffer and heated in boiling water for 5 min, and then 20 μL of each boiled sample was loaded into the respective wells of a 10% polyacrylamide gel. Sodium dodecyl sulfate (SDS) polyacrylamide gel electrophoresis was run at 100 V. The proteins were trans-blotted onto a nitrocellulose membrane at 300 mA for 2 h. The trans-blotted membrane was blocked by 5% fat-free milk in TBST (Tris buffer, pH 7.6 with 0.5% Tween-20) for 1 h at room temperature and then incubated with the primary antibody of iC3b (diluted 1:500 in blocking buffer) at 4 °C overnight. After three washes with TBST, the membrane was incubated with horseradish peroxide conjugated secondary antibody (diluted 1:2000 in blocking buffer) for 1 h at room temperature. After three washes with TBST, the protein bands were detected using an ECL reagent kit and imaged with an Amersham Imager 600 (GE Healthcare, Singapore).

ASSOCIATED CONTENT

Supporting Information

The Supporting Information is available free of charge on the ACS Publications website at DOI: 10.1021/acsnano.6b05409.

More detailed information is provided about AFM and FTIR characterization of graphene oxide sheets (Figures S1 and S2), measurement of bulk protein concentration (Figure S3), fluorescence microscopy control experiments (Figures S4 and S5), and SDS-PAGE/Western Blot analysis (Figure S6) (PDF)

AUTHOR INFORMATION

Corresponding Author

*E-mail: njcho@ntu.edu.sg.

Author Contributions

#J.N.B. and J.A.J. contributed equally to this work.

Notes

The authors declare no competing financial interest.

ACKNOWLEDGMENTS

N.-J.C. acknowledges support from the National Research Foundation of Singapore through a Competitive Research Programme grant (NRF-CRP10-2012-07) as well as from Nanyang Technological University through a start-up grant (M4080751.070). P.S.W. acknowledges support from the National Science Foundation (No. 1509794). We thank S. Kim, H. Jung, and W. Ng for technical assistance with materials characterization.

REFERENCES

(1) Mao, H. Y.; Laurent, S.; Chen, W.; Akhavan, O.; Imani, M.; Ashkarran, A. A.; Mahmoudi, M. Graphene: Promises, Facts, Opportunities, and Challenges in Nanomedicine. *Chem. Rev.* **2013**, *113*, 3407−3424.

(2) Chung, C.; Kim, Y.-K.; Shin, D.; Ryoo, S.-R.; Hong, B. H.; Min, D.-H. Biomedical Applications of Graphene and Graphene Oxide. *Acc. Chem. Res.* **2013**, *46*, 2211−2224.

(3) Bitounis, D.; Ali-Boucetta, H.; Hong, B. H.; Min, D. H.; Kostarelos, K. Prospects and Challenges of Graphene in Biomedical Applications. *Adv. Mater.* **2013**, *25*, 2258−2268.

(4) Marchesan, S.; Melchionna, M.; Prato, M. Wire Up on Carbon Nanostructures! How To Play a Winning Game. *ACS Nano* **2015**, *9*, 9441−9450.

(5) Yan, L.; Zheng, Y. B.; Zhao, F.; Li, S.; Gao, X.; Xu, B.; Weiss, P. S.; Zhao, Y. Chemistry and Physics of a Single Atomic Layer:

DOI: 10.1021/acsnano.6b05409
ACS Nano 2016, 10, 10161−10172

Strategies and Challenges for Functionalization of Graphene and Graphene-Based Materials. *Chem. Soc. Rev.* **2012**, *41*, 97−114.
(6) Chen, D.; Feng, H.; Li, J. Graphene Oxide: Preparation, Functionalization, and Electrochemical Applications. *Chem. Rev.* **2012**, *112*, 6027−6053.
(7) Georgakilas, V.; Tiwari, J. N.; Kemp, K. C.; Perman, J. A.; Bourlinos, A. B.; Kim, K. S.; Zboril, R. Noncovalent Functionalization of Graphene and Graphene Oxide for Energy Materials, Biosensing, Catalytic, and Biomedical Applications. *Chem. Rev.* **2016**, *116*, 5464−5519.
(8) Kostarelos, K.; Novoselov, K. S. Exploring the Interface of Graphene and Biology. *Science* **2014**, *344*, 261−263.
(9) McCallion, C.; Burthem, J.; Rees-Unwin, K.; Golovanov, A.; Pluen, A. Graphene in Therapeutics Delivery: Problems, Solutions and Future Opportunities. *Eur. J. Pharm. Biopharm.* **2016**, *104*, 235−250.
(10) Dudek, I.; Skoda, M.; Jarosz, A.; Szukiewicz, D. The Molecular Influence of Graphene and Graphene Oxide on the Immune System under *In Vitro* and *In Vivo* Conditions. *Arch. Immunol. Ther. Exp.* **2016**, *64*, 195−215.
(11) Orecchioni, M.; Ménard-Moyon, C.; Delogu, L. G.; Bianco, A. Graphene and the Immune System: Challenges and Potentiality. *Adv. Drug Delivery Rev.* **2016**, *105*, 163−175.
(12) Sydlik, S. A.; Jhunjhunwala, S.; Webber, M. J.; Anderson, D. G.; Langer, R. *In Vivo* Compatibility of Graphene Oxide with Differing Oxidation States. *ACS Nano* **2015**, *9*, 3866−3874.
(13) Ricklin, D.; Hajishengallis, G.; Yang, K.; Lambris, J. D. Complement: A Key System for Immune Surveillance and Homeostasis. *Nat. Immunol.* **2010**, *11*, 785−797.
(14) Moghimi, S. M.; Andersen, A. J.; Ahmadvand, D.; Wibroe, P. P.; Andresen, T. L.; Hunter, A. C. Material Properties in Complement Activation. *Adv. Drug Delivery Rev.* **2011**, *63*, 1000−1007.
(15) Moghimi, S. M.; Farhangrazi, Z. S. Nanomedicine and the Complement Paradigm. *Nanomedicine (N. Y., NY, U. S.)* **2013**, *9*, 458−460.
(16) Szebeni, J. Complement Activation by Nanomaterials. In *Handbook of Safety Assessment of Nanomaterials: From Toxicological Testing to Personalized Medicine*; Bengt, F., Ed.; Pan Stanford Publishing, 2015; pp 281−310.
(17) Szeto, G. L.; Lavik, E. B. Materials Design at the Interface of Nanoparticles and Innate Immunity. *J. Mater. Chem. B* **2016**, *4*, 1610−1618.
(18) Zhang, X.-Q.; Xu, X.; Bertrand, N.; Pridgen, E.; Swami, A.; Farokhzad, O. C. Interactions of Nanomaterials and Biological Systems: Implications to Personalized Nanomedicine. *Adv. Drug Delivery Rev.* **2012**, *64*, 1363−1384.
(19) Szebeni, J. Complement Activation-Related Pseudoallergy: A Stress Reaction in Blood Triggered by Nanomedicines and Biologicals. *Mol. Immunol.* **2014**, *61*, 163−173.
(20) Sarma, J. V.; Ward, P. A. The Complement System. *Cell Tissue Res.* **2011**, *343*, 227−235.
(21) Rus, H.; Cudrici, C.; Niculescu, F. The Role of the Complement System in Innate Immunity. *Immunol. Res.* **2005**, *33*, 103−112.
(22) Nilsson, B.; Ekdahl, K. N.; Mollnes, T. E.; Lambris, J. D. The Role of Complement in Biomaterial-Induced Inflammation. *Mol. Immunol.* **2007**, *44*, 82−94.
(23) Lachmann, P. J. The Amplification Loop of the Complement Pathways. *Adv. Immunol.* **2009**, *104*, 115−149.
(24) Wei, X.-Q.; Hao, L.-Y.; Shao, X.-R.; Zhang, Q.; Jia, X.-Q.; Zhang, Z.-R.; Lin, Y.-F.; Peng, Q. Insight into the Interaction of Graphene Oxide with Serum Proteins and the Impact of the Degree of Reduction and Concentration. *ACS Appl. Mater. Interfaces* **2015**, *7*, 13367−13374.
(25) Wibroe, P. P.; Petersen, S. V.; Bovet, N.; Laursen, B. W.; Moghimi, S. M. Soluble and Immobilized Graphene Oxide Activates Complement System Differently Dependent on Surface Oxidation State. *Biomaterials* **2016**, *78*, 20−26.
(26) Nilsson, B.; Korsgren, O.; Lambris, J. D.; Ekdahl, K. N. Can Cells and Biomaterials in Therapeutic Medicine be Shielded from Innate Immune Recognition? *Trends Immunol.* **2010**, *31*, 32−38.
(27) Yu, K.; Mei, Y.; Hadjesfandiari, N.; Kizhakkedathu, J. N. Engineering Biomaterials Surfaces to Modulate the Host Response. *Colloids Surf., B* **2014**, *124*, 69−79.
(28) Meng, C.; Zhi, X.; Li, C.; Li, C.; Chen, Z.; Qiu, X.; Ding, C.; Ma, L.; Lu, H.; Chen, D. Graphene Oxides Decorated with Carnosine as an Adjuvant To Modulate Innate Immune and Improve Adaptive Immunity *In Vivo*. *ACS Nano* **2016**, *10*, 2203−2213.
(29) Xu, M.; Zhu, J.; Wang, F.; Xiong, Y.; Wu, Y.; Wang, Q.; Weng, J.; Zhang, Z.; Chen, W.; Liu, S. Improved *In Vitro* and *In Vivo* Biocompatibility of Graphene Oxide through Surface Modification: Poly(Acrylic Acid)-Functionalization is Superior to PEGylation. *ACS Nano* **2016**, *10*, 3267−3281.
(30) Tan, X.; Feng, L.; Zhang, J.; Yang, K.; Zhang, S.; Liu, Z.; Peng, R. Functionalization of Graphene Oxide Generates a Unique Interface for Selective Serum Protein Interactions. *ACS Appl. Mater. Interfaces* **2013**, *5*, 1370−1377.
(31) Moghimi, S. M.; Andersen, A. J.; Hashemi, S. H.; Lettiero, B.; Ahmadvand, D.; Hunter, A.; Andresen, T. L.; Hamad, I.; Szebeni, J. Complement Activation Cascade Triggered by PEG−PL Engineered Nanomedicines and Carbon Nanotubes: The Challenges Ahead. *J. Controlled Release* **2010**, *146*, 175−181.
(32) Ekdahl, K. N.; Lambris, J. D.; Elwing, H.; Ricklin, D.; Nilsson, P. H.; Teramura, Y.; Nicholls, I. A.; Nilsson, B. Innate Immunity Activation on Biomaterial Surfaces: A Mechanistic Model and Coping Strategies. *Adv. Drug Delivery Rev.* **2011**, *63*, 1042−1050.
(33) Andersen, A. J.; Wibroe, P. P.; Moghimi, S. M. Perspectives on Carbon Nanotube-Mediated Adverse Immune Effects. *Adv. Drug Delivery Rev.* **2012**, *64*, 1700−1705.
(34) Andersen, A. J.; Windschiegl, B.; Ilbasmis-Tamer, S.; Degim, I. T.; Hunter, A. C.; Andresen, T. L.; Moghimi, S. M. Complement Activation by PEG-Functionalized Multi-Walled Carbon Nanotubes is Independent of PEG Molecular Mass and Surface Density. *Nanomedicine (N. Y., NY, U. S.)* **2013**, *9*, 469−473.
(35) Peng, Q.; Mu, H. The Potential of Protein−Nanomaterial Interaction for Advanced Drug Delivery. *J. Controlled Release* **2016**, *225*, 121−132.
(36) Lynch, I.; Dawson, K. A. Protein-Nanoparticle Interactions. *Nano Today* **2008**, *3*, 40−47.
(37) Monopoli, M. P.; Åberg, C.; Salvati, A.; Dawson, K. A. Biomolecular Coronas Provide the Biological Identity of Nanosized Materials. *Nat. Nanotechnol.* **2012**, *7*, 779−786.
(38) Pino, P.; Pelaz, B.; Zhang, Q.; Maffre, P.; Nienhaus, G. U.; Parak, W. J. Protein Corona Formation Around Nanoparticles−from the Past to the Future. *Mater. Horiz.* **2014**, *1*, 301−313.
(39) Ge, C.; Tian, J.; Zhao, Y.; Chen, C.; Zhou, R.; Chai, Z. Towards Understanding of Nanoparticle−Protein Corona. *Arch. Toxicol.* **2015**, *89*, 519−539.
(40) Hu, W.; Peng, C.; Lv, M.; Li, X.; Zhang, Y.; Chen, N.; Fan, C.; Huang, Q. Protein Corona-Mediated Mitigation of Cytotoxicity of Graphene Oxide. *ACS Nano* **2011**, *5*, 3693−3700.
(41) Mu, Q.; Su, G.; Li, L.; Gilbertson, B. O.; Yu, L. H.; Zhang, Q.; Sun, Y.-P.; Yan, B. Size-Dependent Cell Uptake of Protein-Coated Graphene Oxide Nanosheets. *ACS Appl. Mater. Interfaces* **2012**, *4*, 2259−2266.
(42) Salvador-Morales, C.; Flahaut, E.; Sim, E.; Sloan, J.; Green, M. L.; Sim, R. B. Complement Activation and Protein Adsorption by Carbon Nanotubes. *Mol. Immunol.* **2006**, *43*, 193−201.
(43) Salvador-Morales, C.; Basiuk, E. V.; Basiuk, V. A.; Green, M. L.; Sim, R. B. Effects of Covalent Functionalization on the Biocompatibility Characteristics of Multi-Walled Carbon Nanotubes. *J. Nanosci. Nanotechnol.* **2008**, *8*, 2347−2356.
(44) Rybak-Smith, M. J.; Pondman, K. M.; Flahaut, E.; Salvador-Morales, C.; Sim, R. B. Recognition of Carbon Nanotubes by the Human Innate Immune System. *Carbon Nanotubes for Biomedical Applications*; Springer, 2011; pp 183−210.
(45) Rybak-Smith, M. J.; Sim, R. B. Complement Activation by Carbon Nanotubes. *Adv. Drug Delivery Rev.* **2011**, *63*, 1031−1041.
(46) Rybak-Smith, M. J.; Tripisciano, C.; Borowiak-Palen, E.; Lamprecht, C.; Sim, R. B. Effect of Functionalization of Carbon

DOI: 10.1021/acsnano.6b05409
ACS Nano 2016, 10, 10161−10172

Nanotubes with Psychosine on Complement Activation and Protein Adsorption. *J. Biomed. Nanotechnol.* **2011**, *7*, 830−839.
(47) Andersen, A. J.; Robinson, J. T.; Dai, H.; Hunter, A. C.; Andresen, T. L.; Moghimi, S. M. Single-Walled Carbon Nanotube Surface Control of Complement Recognition and Activation. *ACS Nano* **2013**, *7*, 1108−1119.
(48) Pondman, K. M.; Pednekar, L.; Paudyal, B.; Tsolaki, A. G.; Kouser, L.; Khan, H. A.; Shamji, M. H.; ten Haken, B.; Stenbeck, G.; Sim, R. B. Innate Immune Humoral Factors, C1q and Factor H, with Differential Pattern Recognition Properties, Alter Macrophage Response to Carbon Nanotubes. *Nanomedicine (N. Y., NY, U. S.)* **2015**, *11*, 2109−2118.
(49) Chong, Y.; Ge, C.; Yang, Z.; Garate, J. A.; Gu, Z.; Weber, J. K.; Liu, J.; Zhou, R. Reduced Cytotoxicity of Graphene Nanosheets Mediated by Blood-Protein Coating. *ACS Nano* **2015**, *9*, 5713−5724.
(50) Ferreira, V. P.; Pangburn, M. K.; Cortés, C. Complement Control Protein Factor H: The Good, the Bad, and the Inadequate. *Mol. Immunol.* **2010**, *47*, 2187−2197.
(51) Kopp, A.; Hebecker, M.; Svobodová, E.; Józsi, M. Factor H: A Complement Regulator in Health and Disease, and a Mediator of Cellular Interactions. *Biomolecules* **2012**, *2*, 46−75.
(52) Andersson, J.; Larsson, R.; Richter, R.; Ekdahl, K. N.; Nilsson, B. Binding of a Model Regulator of Complement Activation (RCA) to a Biomaterial Surface: Surface-Bound Factor H Inhibits Complement Activation. *Biomaterials* **2001**, *22*, 2435−2443.
(53) Andersson, J.; Bexborn, F.; Klinth, J.; Nilsson, B.; Ekdahl, K. N. Surface-Attached PEO in the Form of Activated Pluronic with Immobilized Factor H Reduces Both Coagulation and Complement Activation in a Whole-Blood Model. *J. Biomed. Mater. Res., Part A* **2006**, *76A*, 25−34.
(54) Li, Y.; Qiu, W.; Zhang, L.; Fung, J.; Lin, F. Painting Factor H onto Mesenchymal Stem Cells Protects the Cells from Complement- and Neutrophil-Mediated Damage. *Biomaterials* **2016**, *102*, 209−219.
(55) Wu, Y.-Q.; Qu, H.; Sfyroera, G.; Tzekou, A.; Kay, B. K.; Nilsson, B.; Ekdahl, K. N.; Ricklin, D.; Lambris, J. D. Protection of Nonself Surfaces from Complement Attack by Factor H-Binding Peptides: Implications for Therapeutic Medicine. *J. Immunol.* **2011**, *186*, 4269−4277.
(56) Nilsson, P. H.; Ekdahl, K. N.; Magnusson, P. U.; Qu, H.; Iwata, H.; Ricklin, D.; Hong, J.; Lambris, J. D.; Nilsson, B.; Teramura, Y. Autoregulation of Thromboinflammation on Biomaterial Surfaces by a Multicomponent Therapeutic Coating. *Biomaterials* **2013**, *34*, 985−994.
(57) Moghimi, S. M.; Trippler, K. C.; Simberg, D. The Art of Complement: Complement Sensing of Nanoparticles and Consequences. In *Nanomedicine*; Howard, K., Peer, D., Vorup-Jensen, T., Eds.; Springer, 2016; pp 43−51.
(58) Andersson, J.; Ekdahl, K. N.; Lambris, J. D.; Nilsson, B. Binding of C3 Fragments on Top of Adsorbed Plasma Proteins During Complement Activation on a Model Biomaterial Surface. *Biomaterials* **2005**, *26*, 1477−1485.
(59) Fadeel, B.; Feliu, N.; Vogt, C.; Abdelmonem, A. M.; Parak, W. J. Bridge Over Troubled Waters: Understanding the Synthetic and Biological Identities of Engineered Nanomaterials. *Wiley Interdiscip. Rev.: Nanomed. Nanobiotechnol.* **2013**, *5*, 111−129.
(60) Pelaz, B.; del Pino, P.; Maffre, P.; Hartmann, R.; Gallego, M.; Rivera-Fernandez, S.; de la Fuente, J. M.; Nienhaus, G. U.; Parak, W. J. Surface Functionalization of Nanoparticles with Polyethylene Glycol: Effects on Protein Adsorption and Cellular Uptake. *ACS Nano* **2015**, *9*, 6996−7008.
(61) Saha, K.; Rahimi, M.; Yazdani, M.; Kim, S. T.; Moyano, D. F.; Hou, S.; Das, R.; Mout, R.; Rezaee, F.; Mahmoudi, M.; Rotello, V. M. Regulation of Macrophage Recognition through the Interplay of Nanoparticle Surface Functionality and Protein Corona. *ACS Nano* **2016**, *10*, 4421−4430.
(62) Palchetti, S.; Pozzi, D.; Mahmoudi, M.; Caracciolo, G. Exploitation of Nanoparticle−Protein Corona for Emerging Therapeutic and Diagnostic Applications. *J. Mater. Chem. B* **2016**, *4*, 4376−4381.
(63) Schöttler, S.; Becker, G.; Winzen, S.; Steinbach, T.; Mohr, K.; Landfester, K.; Mailänder, V.; Wurm, F. R. Protein Adsorption is Required for Stealth Effect of Poly (Ethylene Glycol)-and Poly (Phosphoester)-Coated Nanocarriers. *Nat. Nanotechnol.* **2016**, *11*, 372−377.
(64) Liu, J.; Fu, S.; Yuan, B.; Li, Y.; Deng, Z. Toward a Universal "Adhesive Nanosheet" for the Assembly of Multiple Nanoparticles Based on a Protein-Induced Reduction/Decoration of Graphene Oxide. *J. Am. Chem. Soc.* **2010**, *132*, 7279−7281.
(65) Kuchlyan, J.; Kundu, N.; Banik, D.; Roy, A.; Sarkar, N. Spectroscopy and Fluorescence Lifetime Imaging Microscopy To Probe the Interaction of Bovine Serum Albumin with Graphene Oxide. *Langmuir* **2015**, *31*, 13793−13801.
(66) Kenry; Loh, K. P.; Lim, C. T. Molecular Interactions of Graphene Oxide with Human Blood Plasma Proteins. *Nanoscale* **2016**, *8*, 9425−9441.
(67) Li, S.; Aphale, A. N.; Macwan, I. G.; Patra, P. K.; Gonzalez, W. G.; Miksovska, J.; Leblanc, R. M. Graphene Oxide as a Quencher for Fluorescent Assay of Amino Acids, Peptides, and Proteins. *ACS Appl. Mater. Interfaces* **2012**, *4*, 7069−7075.
(68) Ding, Z.; Ma, H.; Chen, Y. Interaction of Graphene Oxide with Human Serum Albumin and Its Mechanism. *RSC Adv.* **2014**, *4*, 55290−55295.
(69) Gu, Z.; Yang, Z.; Wang, L.; Zhou, H.; Jimenez-Cruz, C. A.; Zhou, R. The Role of Basic Residues in the Adsorption of Blood Proteins onto the Graphene Surface. *Sci. Rep.* **2015**, *5*, 10873−10873.
(70) Li, D.; Mueller, M. B.; Gilje, S.; Kaner, R. B.; Wallace, G. G. Processable Aqueous Dispersions of Graphene Nanosheets. *Nat. Nanotechnol.* **2008**, *3*, 101−105.
(71) Lai, Q.; Zhu, S.; Luo, X.; Zou, M.; Huang, S. Ultraviolet-Visible Spectroscopy of Graphene Oxides. *AIP Adv.* **2012**, *2*, 032146.
(72) Guerrero-Contreras, J.; Caballero-Briones, F. Graphene Oxide Powders with Different Oxidation Degree, Prepared by Synthesis Variations of the Hummers Method. *Mater. Chem. Phys.* **2015**, *153*, 209−220.
(73) Trusovas, R.; Račiukaitis, G.; Niaura, G.; Barkauskas, J.; Valušis, G.; Pauliukaite, R. Recent Advances in Laser Utilization in the Chemical Modification of Graphene Oxide and Its Applications. *Adv. Opt. Mater.* **2016**, *4*, 37−65.
(74) Moreno-Castilla, C.; Lopez-Ramon, M.; Carrasco-Marın, F. Changes in Surface Chemistry of Activated Carbons by Wet Oxidation. *Carbon* **2000**, *38*, 1995−2001.
(75) Fuente, E.; Menendez, J.; Diez, M.; Suarez, D.; Montes-Moran, M. Infrared Spectroscopy of Carbon Materials: A Quantum Chemical Study of Model Compounds. *J. Phys. Chem. B* **2003**, *107*, 6350−6359.
(76) Wu, C.; He, Q.; Zhu, A.; Yang, H.; Liu, Y. Probing the Protein Conformation and Adsorption Behaviors in Nanographene Oxide-Protein Complexes. *J. Nanosci. Nanotechnol.* **2014**, *14*, 2591−2598.
(77) Li, H.; Fierens, K.; Zhang, Z.; Vanparijs, N.; Schuijs, M. J.; Van Steendam, K.; Feiner Gracia, N. l.; De Rycke, R.; De Beer, T.; De Beuckelaer, A. Spontaneous Protein Adsorption on Graphene Oxide Nanosheets Allowing Efficient Intracellular Vaccine Protein Delivery. *ACS Appl. Mater. Interfaces* **2016**, *8*, 1147−1155.
(78) Konkena, B.; Vasudevan, S. Understanding Aqueous Dispersibility of Graphene Oxide and Reduced Graphene Oxide through pK_a Measurements. *J. Phys. Chem. Lett.* **2012**, *3*, 867−872.
(79) Des Prez, R.; Bryan, C.; Hawiger, J.; Colley, D. Function of the Classical and Alternate Pathways of Human Complement in Serum Treated with Ethylene Glycol Tetraacetic Acid and $MgCl_2$-Ethylene Glycol Tetraacetic Acid. *Infect. Immun.* **1975**, *11*, 1235−1243.
(80) Nilsson, B.; Svensson, K.-E.; Inganäs, M.; Nilsson, U. A Simplified Assay for the Detection of C3a in Human Plasma Employing a Monoclonal Antibody Raised Against Denatured C3. *J. Immunol. Methods* **1988**, *107*, 281−287.
(81) Sturfelt, G.; Truedsson, L. Complement and Its Breakdown Products in SLE. *Rheumatology* **2005**, *44*, 1227−1232.
(82) Götze, O.; Müller-Eberhard, H. The Alternative Pathway of Complement Activation. *Adv. Immunol.* **1976**, *24*, 1−35.

DOI: 10.1021/acsnano.6b05409
ACS Nano 2016, 10, 10161−10172

(83) Hofer, J.; Forster, F.; Isenman, D. E.; Wahrmann, M.; Leitner, J.; Hölzl, M. A.; Kovarik, J. J.; Stockinger, H.; Böhmig, G. A.; Steinberger, P. Ig-like Transcript 4 as a Cellular Receptor for Soluble Complement Fragment C4d. *FASEB J.* **2016**, *30*, 1492−1503.
(84) Rabe, M.; Verdes, D.; Seeger, S. Understanding Protein Adsorption Phenomena at Solid Surfaces. *Adv. Colloid Interface Sci.* **2011**, *162*, 87−106.
(85) de Córdoba, S. R.; Esparza-Gordillo, J.; de Jorge, E. G.; Lopez-Trascasa, M.; Sánchez-Corral, P. The Human Complement Factor H: Functional Roles, Genetic Variations and Disease Associations. *Mol. Immunol.* **2004**, *41*, 355−367.
(86) Morgan, H. P.; Schmidt, C. Q.; Guariento, M.; Blaum, B. S.; Gillespie, D.; Herbert, A. P.; Kavanagh, D.; Mertens, H. D.; Svergun, D. I.; Johansson, C. M. Structural Basis for Engagement by Complement Factor H of C3b on a Self Surface. *Nat. Struct. Mol. Biol.* **2011**, *18*, 463−470.
(87) Mastellos, D. C.; Yancopoulou, D.; Kokkinos, P.; Huber-Lang, M.; Hajishengallis, G.; Biglarnia, A. R.; Lupu, F.; Nilsson, B.; Risitano, A. M.; Ricklin, D. Compstatin: a C3-targeted Complement Inhibitor Reaching Its Prime for Bedside Intervention. *Eur. J. Clin. Invest.* **2015**, *45*, 423−440.
(88) Ricklin, D.; Lambris, J. D. Therapeutic Control of Complement Activation at the Level of the Central Component C3. *Immunobiology* **2016**, *221*, 740−746.
(89) Kong, H.; Wang, L.; Zhu, Y.; Huang, Q.; Fan, C. Culture Medium-Associated Physicochemical Insights on the Cytotoxicity of Carbon Nanomaterials. *Chem. Res. Toxicol.* **2015**, *28*, 290−295.
(90) Yu, K.; Lai, B. F.; Foley, J. H.; Krisinger, M. J.; Conway, E. M.; Kizhakkedathu, J. N. Modulation of Complement Activation and Amplification on Nanoparticle Surfaces by Glycopolymer Conformation and Chemistry. *ACS Nano* **2014**, *8*, 7687−7703.
(91) Salvati, A.; Pitek, A. S.; Monopoli, M. P.; Prapainop, K.; Bombelli, F. B.; Hristov, D. R.; Kelly, P. M.; Åberg, C.; Mahon, E.; Dawson, K. A. Transferrin-Functionalized Nanoparticles Lose Their Targeting Capabilities When a Biomolecule Corona Adsorbs on the Surface. *Nat. Nanotechnol.* **2013**, *8*, 137−143.
(92) Caracciolo, G.; Palchetti, S.; Colapicchioni, V.; Digiacomo, L.; Pozzi, D.; Capriotti, A. L.; La Barbera, G.; Laganà, A. Stealth Effect of Biomolecular Corona on Nanoparticle Uptake by Immune Cells. *Langmuir* **2015**, *31*, 10764−10773.
(93) Mirshafiee, V.; Kim, R.; Park, S.; Mahmoudi, M.; Kraft, M. L. Impact of Protein Pre-Coating on the Protein Corona Composition and Nanoparticle Cellular Uptake. *Biomaterials* **2016**, *75*, 295−304.
(94) Hebecker, M.; Alba-Domínguez, M.; Roumenina, L. T.; Reuter, S.; Hyvärinen, S.; Dragon-Durey, M.-A.; Jokiranta, T. S.; Sánchez-Corral, P.; Józsi, M. An Engineered Construct Combining Complement Regulatory and Surface-Recognition Domains Represents a Minimal-Size Functional Factor H. *J. Immunol.* **2013**, *191*, 912−921.
(95) Mészáros, T.; Csincsi, Á. I.; Uzonyi, B.; Hebecker, M.; Fülöp, T. G.; Erdei, A.; Szebeni, J.; Józsi, M. Factor H Inhibits Complement Activation Induced by Liposomal and Micellar Drugs and the Therapeutic Antibody Rituximab. *Nanomedicine (N. Y., NY, U. S.)* **2016**, *12*, 1023−1031.
(96) Nichols, E.-M.; Barbour, T. D.; Pappworth, I. Y.; Wong, E. K.; Palmer, J. M.; Sheerin, N. S.; Pickering, M. C.; Marchbank, K. J. An Extended Mini-Complement Factor H Molecule Ameliorates Experimental C3 Glomerulopathy. *Kidney Int.* **2015**, *88*, 1314−1322.

DOI: 10.1021/acsnano.6b05409
ACS Nano 2016, 10, 10161−10172